

Electron microscopic observations of Bi and Tl bearing cuprate high temperature superconductors

B DAS, K RAMAKRISHNA, G D VERMA, R S TIWARI and O N SRIVASTAVA

Department of Physics, Banaras Hindu University, Varanasi 221005, India

Abstract. The second generation of high temperature superconductors typified by $\text{Bi}_2\text{Sr}_2\text{Ca}_{n-1}\text{Cu}_n\text{O}_{2n+4}$ and $\text{Tl}_2\text{Ba}_2\text{Ca}_{n-1}\text{Cu}_n\text{O}_{2n+4}$ exhibits curious structural properties which have direct relevance to the superconducting behaviour particularly transition temperature (T_c). The present paper reports on investigations of structural properties at microlevel in Bi-bearing HTCS. We have found curious structural characteristics which manifests itself in the form of transformation from $a_p \times a_p \times c$ to $(2)^{1/2}a_p \times (2)^{1/2}a_p \times c$ through the loss of calcium atoms and the formation of five-fold modulated phase along b through the loss of Ca and Sr atoms. We have also found the evidence of high periodicities ($n=4$) $\text{Bi}_2\text{Sr}_2\text{Ca}_3\text{Cu}_4\text{O}_{12}$. The microstructural characteristics of HTCS showing the higher $T_c(R=0) \sim 120$ K exhibits unusual characteristics.

Keywords. High periodic structures; cation deficiency; modified synthesis; planar faults.

1. Crystallographic characteristics and stoichiometric considerations of Bi–Sr–Ca–Cu–O HTSC materials

The case of the high temperature superconductor $\text{Bi}_2\text{Sr}_2\text{Ca}_1\text{Cu}_2\text{O}_8$ in regard to its crystallographic and chemical characteristics seems curious. The high T_c material—unlike its predecessor $\text{YBa}_2\text{Cu}_3\text{O}_{7-x}$ is not sensitive to oxygen treatment and stoichiometry (Maeda *et al* 1988; Tarascon *et al* 1988). It is generally believed that Cu^{3+} is essential for superconductivity to occur. This can be accomplished by the deficiency of some cations other than the Cu ion. The deficiency of non-copper cations appears to be the only way to turn some of the Cu^{2+} into Cu^{3+} in the $\text{Bi}_2\text{Sr}_2\text{Ca}_1\text{Cu}_2\text{O}_8$ (Zandbergen *et al* 1988; Chippindale *et al* 1988; Cheetam *et al* 1988). On the other hand, the stabilization of modified perovskite-like structure with $a = (2)^{1/2}a_p$, $b = (2)^{1/2}a_p$ and $c = 8a_p$ (where a_p is the lattice parameter of basic perovskite cell), the occurrence of long-period modulated structures along a and b directions with periodicities of $5 \times (2)^{1/2}a_p$ and the existence of several closely related structures with larger c periodicities, form some of the examples of crystal subtleties in the Bi–Sr–Ca–Cu–O (BCSCO) system. Keeping this in view we have carried out a study aimed at monitoring the stoichiometry of non-copper cations and to examine the relevance of this on the crystallographic characteristics. The stoichiometric and crystallographic characteristics have been examined in regard to the appearance of Cu^{3+} ions.

In order to explore the structural and microstructural characteristics and compositional details transmission electron microscope was used in all the manifestations such as imaging, diffraction and analytical modes (EDAX). The microstructural investigations of different samples revealed that BCSCO system has varied c parameters. The highest c periodicity found is 48 Å. In addition, the various c -periodicities found in the BCSCO are ~ 24.4 Å, 30.34 Å and ~ 37 Å which are at



Figure 1. Selected area diffraction pattern exhibiting the presence of high periodicity and disorder.

intervals of $\sim 6 \text{ \AA}$. In the present investigation evidences for the occurrence of very high periodicity involving disorder have also been found. Figure 1 shows a selected area diffraction (SAD) pattern where a streaking (indicative of disorder) interconnecting the spots corresponding to high periodicity can be seen. Extensive investigation reveals that the BCSCO phase embodies a pseudotetragonal system with lattice periodicities $a \approx b \approx (2)^{1/2}a_p$ (5.41 \AA). Not only that, this system further has been modulated incommensurately along the b -direction with new cell dimensions $(2)^{1/2}a_p \times 5(2)^{1/2}a_p \times 8a_p$. The stoichiometry of the cations with particular reference to the non-copper cations was monitored through EDAX technique with a PV 9900 system coupled to a Philips EM CM-12 electron microscope. The important result emerging from the above investigation is that whereas the Bi cations did not show any stoichiometric deficiency, the calcium and strontium cations invariably were found to be deficient. It can thus be taken that the as-synthesized $\text{Bi}_2\text{Sr}_2\text{Ca}_1\text{Cu}_2\text{O}_8$ (and similar other members of the series $\text{Bi}_2\text{Sr}_2\text{Ca}_{n-1}\text{Cu}_n\text{O}_{4+2n}$) possess built-in nonstoichiometry in regard to the Ca and Sr atoms.

We have found that as regards the Ca atoms the deficiency arises through a crystallographic transformation. This consists of the transformation of a basic perovskite-like tetragonal unit cell with $a_p \times a_p \times c$ to the modified unit cell with $(2)^{1/2}a_p \times (2)^{1/2}a_p \times c$ (termed as $T(2)^{1/2}a_p$). The $T_{a_p} \rightarrow T(2)^{1/2}a_p$ (see figure 2) transformation is thought to take place with annealing at close to the melting point. The occurrence of Ca deficiency leading to its effective weight as $\text{Ca}_{0.75}$ would compel some of the Cu^{2+} to change to Cu^{3+} . We next consider the case of Sr deficiency. Similar to calcium, the deficiency of the other alkaline earth component i.e. strontium atoms can also lead to the transition $\text{Cu}^{2+} \rightarrow \text{Cu}^{3+}$. An interesting consequence which follows is that the ordered Sr vacancies may, besides resulting in the transition $\text{Cu}^{2+} \rightarrow \text{Cu}^{3+}$ may also lead to the formation of the known superstructure with the

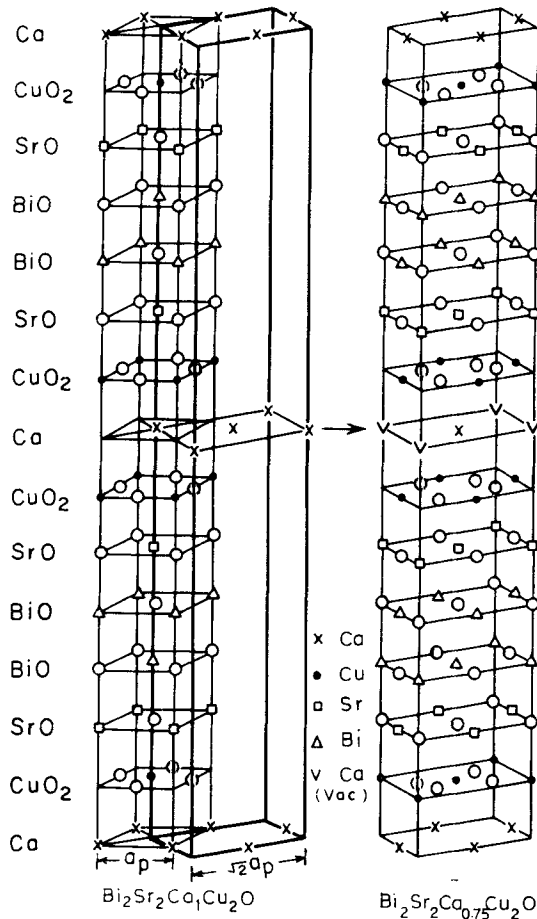


Figure 2. Schematic representation of the projection of the initial and proposed transformed structure on the bc plane. Here the transformation $a_p \times a_p \times c \rightarrow (2)^{1/2}a_p \times (2)^{1/2}a_p \times c$ is due to the deficiency of Ca atoms only.

b periodicity being 5 times that of original unit cell (see figure 3). Thus the two deficiencies taken together lead to several effective Cu valencies and crystallographic transformations ($Ta_p \rightarrow T(2)^{1/2}a_p \rightarrow T5(2)^{1/2}a_p$).

2. Synthesis, crystallographic characteristics and higher T_c onsets in Tl–Ba–Ca–Cu–O superconductor

2.1 Modified synthesis route

The synthesis of the $\text{Tl}_m\text{Ba}_2\text{Ca}_{n-1}\text{Cu}_n\text{O}_{2(n+1)+m}$ is rather complicated due to the instability and toxicity of Tl_2O_3 (Halder *et al* 1988) which decomposes at the synthesis temperatures (850–900°C). The decomposed product Tl_2O melts between 300–400°C resulting in a quite volatile form. This material, therefore needs short annealing time

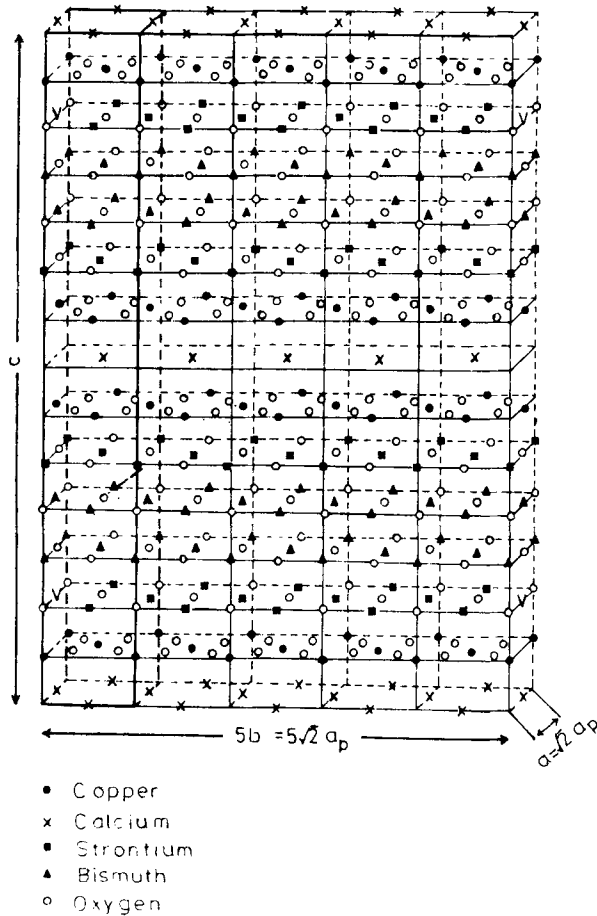


Figure 3. A feasible structural model taking into account the known symmetry of the lattice and Ca, Sr deficiency based on the transformation $(2)^{1/2}a_p \times (2)^{1/2}a_p \times c \rightarrow (2)^{1/2}a_p \times 5(2)^{1/2}a_p \times c$.

as well as excess Tl_2O_3 to compensate for Tl loss and to assist in the formation of a superconducting phase. In order to overcome the above shortcomings, the superconducting $Tl_2Ba_2Ca_{n-1}Cu_nO_{2n+4}$ compounds have been synthesized in the present investigation through solid-state interdiffusion with encapsulation of Tl_2O_3 in the Ba–Ca–Cu–O precursor pellets (Verma *et al* 1989). The encapsulation is carried out by forming pellets with geometrical artifacts providing room for housing Tl_2O_3 between the precursor pellets. Appropriate quantities of $BaCO_3$, $CaCO_3$ and CuO were thoroughly mixed, ground and calcined at $\sim 900^\circ C$ for ~ 36 h, with intermediate grinding. The precursor (Ba–Ca–Cu–O) thus prepared was pressed into a pellet (labelled A in figure 4, 6 mm diameter and 2 mm thickness) having a groove (4 mm diameter and 1 mm deep) as shown in figure 4. The groove size was optimized and the groove filled with an appropriate quantity of Tl_2O_3 powder and another pellet (labelled B, 6 mm diameter and 1 mm thick) of precursor (Ba–Ca–Cu–O) was put above the pellet A and pressed at a pressure of 3–5 ton/inch². The composite pellet was finally fired at $885 \pm 10^\circ C$ under flowing oxygen for 25 min and cooled slowly.

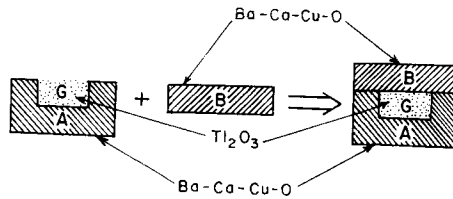


Figure 4. The two parts of the composite pellet labelled as A and B made of precursor matrix (Ba-Ca-Cu-O). Part B has groove for encapsulation of Tl_2O_3 .

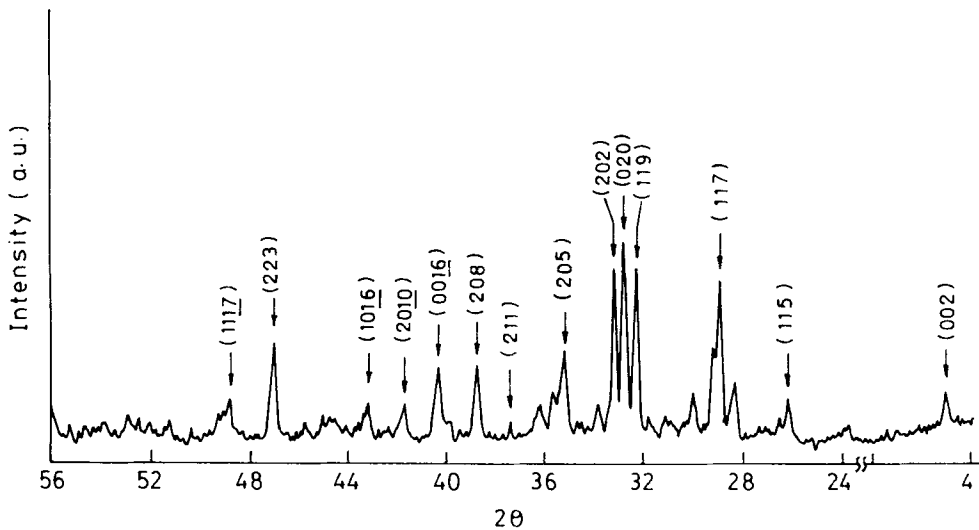


Figure 5. X-ray powder diffraction pattern of $Tl_2Ca_2Ba_2Cu_3O_{10}$ (2223) phase. Nearly all the lines get indexed based on 2223 phase indicating the dominant presence of this phase.

2.2 Crystallographic characteristics and higher T_c onsets in Tl-Ba-Ca-Cu-O superconductors

The phase identification of the as-synthesized composite pellets was carried out by X-ray diffraction using a Philips PW 1710 diffractometer. Figure 5 represents the XRD pattern of part A of the composite pellet, revealing tetragonal phase with $a \approx b \approx 3.821 \text{ \AA}$ and $c \approx 35.645 \text{ \AA}$. The electrical resistance was measured by the four-probe method employing Van der Pauw geometry. The $R-T$ plots of part B and A of the composite pellets are shown in figures 6 and 7 respectively. As can be noted part B pellet has the usual $R-T$ characteristics of Tl: 2212 phase whereas part A exhibited well-defined T_c ($R=0$) at 120 K of Tl:2223 phase.

In order to explore the structural/microstructural characteristics of parts A and B of the composite pellet an electron microscope EM-CM-12 (TEM/STEM) was used. Together with imaging, selected area convergent beam electron diffraction and EDAX technique were used. The SAD patterns taken from part B were usual but the SAD pattern from part A exhibited several abnormalities. Figure 8 exhibits a representative example of $\langle 001 \rangle$ diffraction pattern of part A of the composite pellet, showing

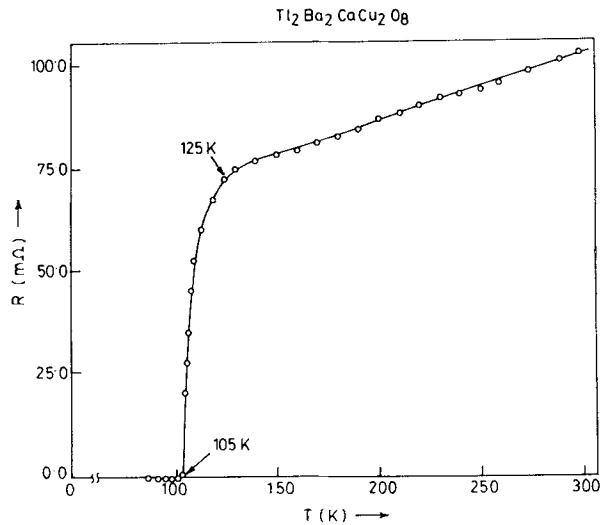


Figure 6. Resistance vs temperature curve of the part B of the composite pellet.

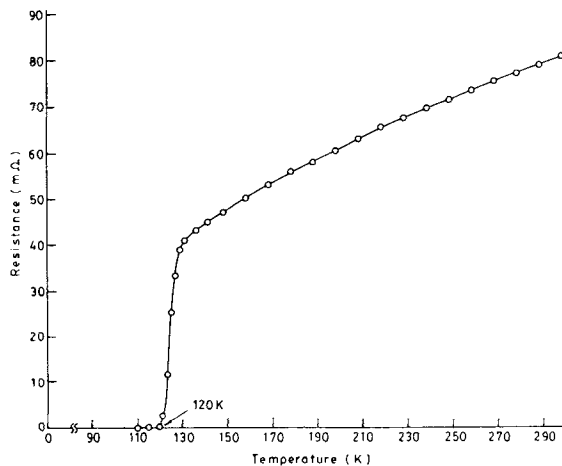
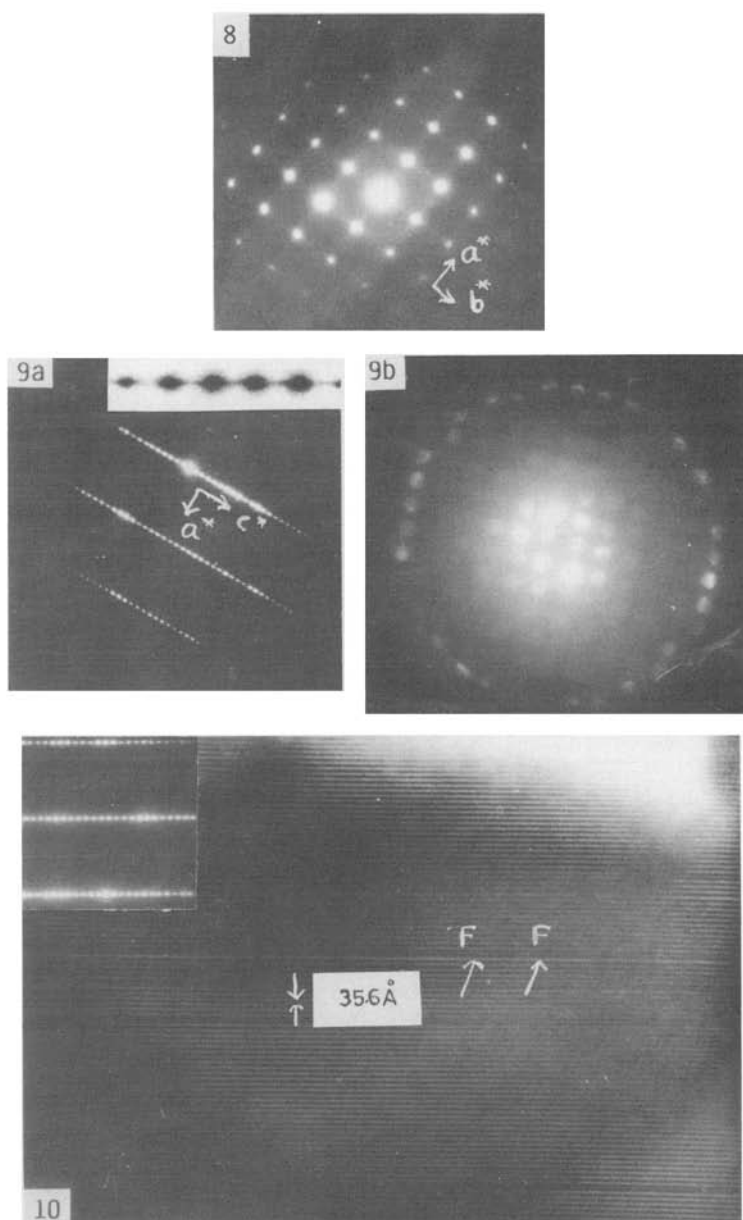


Figure 7. Resistance vs temperature curve of the part A of the composite pellet showing $T_c (R=0)$ at ~ 120 K.

diffuse streaks running parallel to a^*-b^* reciprocal lattice directions. However the origin of the diffuse streaks and its influence on the occurrence of HTSC in part A, is not clear at present. Figure 9(a) shows another SAD pattern in a^*-c^* reciprocal space. The c -periodicity determined from figure 9a was found to be 35-60 Å, thus the part A pellet is of 2223 phase. This was also confirmed by $\langle 001 \rangle$ zone axis pattern exhibiting zero-order and first-order Laue zones (see figure 9b). The inset in figure 9a brings out the sharp diffuse streaking parallel to c^* row. The presence of this streaking apparently reveals the presence of planar disorder representing faults in the stacking along (001) i.e. (Cu-O) planes. A faulted version of the standard structure



Figures 8–10. **8.** $\langle 001 \rangle$ diffraction pattern of part A of the pellet. **9a.** $\langle 100 \rangle$ or $\langle 010 \rangle$ diffraction patterns of part A of the pellet. **9b.** $\langle 001 \rangle$ CBED pattern. **10.** Electron micrograph exhibiting direct lattice resolution.

may correspond to $\text{TlO}-\text{BaO}-\text{Cu}_2\text{O}-\text{Ca}-\text{CuO}_2-\text{Ca}-\text{CuO}_2-\text{BaO}-\text{TlO}$ ----- . A representative micrograph exhibiting the presence of faults is shown in figure 10. In view of these findings it can be said that pellet part A has microregions of the higher members of $2,2,n-1, n$ series i.e. $n > 3$ because higher members of the series are believed to have higher T_c (Perkin *et al* 1988).

Acknowledgement

The authors are grateful to Prof. R P Rastogi for initiating us in this field. They are also thankful to Prof. A R Verma and Prof. Yash Pal for encouragement. Helpful discussions from Drs A V Narlikar, A P B Sinha, Profs T V Ramakrishnan, G V Subba Rao and A A Balchin are gratefully acknowledged. The present work was supported by the University Grants Commission and the Programme Management Board (DST). One of the authors (KR) wishes to thank CSIR, New Delhi for financial support.

References

- Cheetam A K, Chippindale A M and Hibble S J 1988 *Nature (London)* **333** 31
- Chippindale A M, Hibble S J, Hriljac J A, Cowey L, Baggeley D M S, Day P and Cheetam A K 1988 *Physica* **C152** 154
- Halder P et al 1988 *Science* **241** 1198
- Maeda H, Tanaka Y, Fukotomi M and Asano T 1988 *Jpn. J. Appl. Phys. Lett.* **27** 2
- Perkin S S P, Lee V Y, Nazzal A I, Savoy R, Huang T C, Gorman G and Beyers R 1988 *Phys. Rev.* **B38** 6531
- Tarascon J M et al 1988 *Phys. Rev.* **B37** 9382
- Verma G D, Das B and Srivastava O N 1989 *Solid State Commun.* (in press)
- Zandbergen H W, Groen W A, Mijlhoff F C, Tendeloo G and Van Amelinckx S 1988 *Physica* **C156** 325